

Emissions Characteristics of Military Helicopter Engines with JP-8 and Fischer–Tropsch Fuels

Edwin Corporan*

U.S. Air Force Research Laboratory, Wright-Patterson Air Force Base, Ohio 45433

Matthew J. DeWitt, Christopher D. Klingshirn, and Richard Striebich

University of Dayton Research Institute, Dayton, Ohio 45469

and

Meng-Dawn Cheng

Oak Ridge National Laboratory, Oak Ridge, Tennessee 37831

DOI: 10.2514/1.43928

The rapid growth in aviation activities and more stringent U.S. Environmental Protection Agency regulations have increased concerns regarding aircraft emissions, due to their harmful health and environmental impacts, especially in the vicinity of airports and military bases. In this study, the gaseous and particulate-matter emissions of two General Electric T701C engines and one T700 engine were evaluated. The T700 series engines power the U.S. Army's Black Hawk and Apache helicopters. The engines were fueled with standard military JP-8 fuel and were tested at three power settings. In addition, one of the T701C engines was operated on a natural-gas-derived Fischer–Tropsch synthetic paraffinic kerosene jet fuel. Test results show that the T701C engine emits significantly lower particulate-matter emissions than the T700 for all conditions tested. Particulate-matter mass emission indices ranged from 0.2–1.4 g/kg fuel for the T700 and 0.2–0.6 g/kg fuel for the T701C. Slightly higher NO_x and lower CO emissions were observed for the T701C compared with the T700. Operation of the T701C with the Fischer–Tropsch fuel rendered dramatic reductions in soot emissions relative to operation on JP-8, due primarily to the lack of aromatic compounds in the alternative fuel. The Fischer–Tropsch fuel also produced smaller particles and slight reductions in CO emissions.

Introduction

AIRCRAFT have been identified as significant sources of local pollution at airports and military bases. The Federal Aviation Administration (FAA) estimated in 2002 that passenger air travel in the United States would increase about 4% per year [1], further increasing the environmental burden of aircraft and ground support equipment, especially in the vicinity of airports. Even in the absence of any growth in aviation, emissions from aircraft, especially particulate matter (PM), have been under increased scrutiny recently due to their proven harmful health and environmental effects. The more stringent environmental standards imposed by the U.S. Environmental Protection Agency (EPA) will likely impact commercial aviation growth and military operations, including the basing of advanced and legacy aircraft. Therefore, accurate determination of emission indices (EIs) of pollutants from aircraft is necessary to assess their environmental impact to take appropriate corrective action. Robust techniques and instrumentation are needed to perform these challenging measurements from full-scale turbine engines under actual operating conditions. Through several aircraft emissions research projects led by NASA (many in collaboration with the FAA, EPA, U.S. Department of Defense, academia, and industry), significant progress has been made in advancing the knowledge of instrumentation and methodologies for improved reliability of particulate measurements from turbine engines [2,3]. Recently, the SAE E-31 Committee generated an Aerospace Information Report describing instruments and techniques currently available for the measurement of nonvolatile PM emissions [4].

Several instruments that may be employed for these measurements were also assessed under the Strategic Environmental Research and Development Program (SERDP) project CP-1106 [5]. The ultimate goal is to develop methodologies to generate reliable data and reduce the uncertainties associated with existing and future emissions inventories from military and commercial aircraft. In this effort, several of these instruments/techniques were applied to quantify the emissions from the T700 series engines.

In recent years, there has been increased interest in the potential use of alternative jet fuels produced via the Fischer–Tropsch (FT) process for aviation applications. These fuels can be produced domestically from various nonpetroleum feedstocks such as coal, natural gas, and biomass and could therefore reduce reliance on foreign oil. FT fuels are typically comprised solely of iso- and normal paraffins and do not contain heteroatoms, cyclic compounds, or aromatics. Accurate emissions measurements for turbine engines operating with alternative fuels are needed to evaluate their environmental impact. Previous research conducted on turbine engines and combustors have shown significantly reduced PM emissions using FT/JP-8 fuel blends [6–8]. The U.S. Air Force has been very active in the analysis and testing of FT produced fuels and is currently certifying aircraft to operate with a 50/50% by volume FT/JP-8 fuel blend with the goal of certifying all U.S. Air Force weapon systems for use with the alternative fuel blend by 2011. In the present effort, a T701C engine, which powers the U.S. Army's Black Hawk and Apache helicopters, was operated with 100% natural-gas-derived FT fuel and specification JP-8, in order to compare emissions and engine performance. Favorable results from this and other studies will help expedite the certification of engines, aircraft, and ground support equipment for use of synthetic paraffinic kerosene (SPK)-type fuels in commercial and military systems.

T700 and T701C Engines

The General Electric T700-700 or T700-701C (referred to hereafter as T700 and T701C) is the turboshaft engine used to power the UH-60 Black Hawk and AH-64 Apache helicopters. The T701C

Received 19 February 2009; accepted for publication 15 November 2009. This material is declared a work of the U.S. Government and is not subject to copyright protection in the United States. Copies of this paper may be made for personal or internal use, on condition that the copier pay the \$10.00 per-copy fee to the Copyright Clearance Center, Inc., 222 Rosewood Drive, Danvers, MA 01923; include the code 0748-4658/10 and \$10.00 in correspondence with the CCC.

*Senior Research Engineer, Propulsion Directorate; edwin.corporan@wpafb.af.mil.

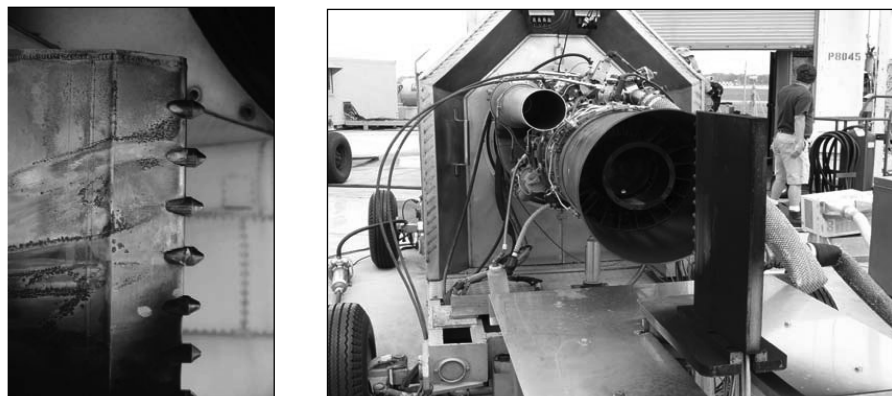


Fig. 1 Particle and gas probes mounted on a water-cooled rake installed 33 cm from the engine exit plane.

is a more powerful and upgraded version of the T700 and is installed in the latest Black Hawk and Apache attack helicopters. They both have six compressor stages and two low- and high-pressure turbines. The overall pressure ratio of the T700 is 17:1 versus 18:1 for the T701C. The T701C has slightly better specific fuel consumption and a higher maximum shaft horsepower than the T700 (1890 vs 1622 shp). The three engines used in this study had a few thousand hours of total operation.

Instrumentation

PM and gaseous emissions instrumentation were transported to the test site and housed during testing in the U.S. Air Force Research Laboratory, Fuels Branch, Turbine Engine Research Transportable Emissions Laboratory (TERTEL). The TERTEL is equipped with state-of-the-art instrumentation for the measurement and analysis of turbine engine emissions. Online analysis of the mostly nonvolatile PM emissions was performed using a TSI, Inc., model 3022A condensation particle counter (CPC) to provide a count of the total particles per unit volume (particle number) via light scattering techniques, and a scanning mobility particle sizer (SMPS) TSI model 3936 was used to measure particle size distributions via electrostatic classification. Basic descriptions of the CPC and SMPS systems can be found elsewhere.[†] The SMPS was composed of a long differential mobility analyzer (DMA) (TSI model 3081) coupled with a condensation particle counter (TSI model 3025). The long DMA was operated at a sheath flow rate of 10 lpm and a sample flow rate of 1.5 lpm, allowing for classification of particles in the range of 7 to 300 nm. An in-house-designed smoke sampler was used to collect PM samples for determination of engine smoke numbers following the techniques in Society of Automotive Engineers (SAE) Aerospace Recommended Practice (ARP) 1179 [9]. In addition, soot samples were collected on quartz filters for offline analysis using a LECO Corporation RC-412 multiphase carbon analyzer. In this method, total carbon mass and the fractions of organic and elemental carbon were inferred via quantitation of the CO₂ generated during the oxidation of volatile and nonvolatile organic species as a function of temperature. Species that oxidize at low temperatures (less than 325°C) are considered volatile organic species [e.g., polycyclic aromatic hydrocarbons (PAHs)], and those that oxidize at higher temperatures are assumed to be primarily elemental carbon (e.g., highly graphitic). The carbon was oxidized to temperatures up to 750°C. The total carbon mass is the sum of the volatile [i.e., organic carbon (OC)] and elemental carbon. Selected soot samples were also analyzed for adsorbed PAH content via ultrasonic extraction and analysis using gas chromatography/mass spectrometry (GC/MS). Direct real-time nonvolatile particle mass concentrations were measured with an Rupprecht & Pataschnick series 1105 tapered-element oscillating microbalance (TEOM). The TEOM measures the mass concentration based on the change in frequency of an oscillating tapered element as PM is deposited on a filter installed at the tip of the element.

Gaseous emissions were quantified using an MKS Instruments, Inc., MultiGas 2030 Fourier transform infrared (FTIR)-based gas analyzer. CO₂ in the diluted sample streams was measured with a nondispersive infrared analyzer. The total unburned hydrocarbons were quantified with an analyzer based on flame ionization detection; however, an instrument malfunction precluded its use for all test cases, and thus the data are not included.

Emissions Sampling System

PM and gaseous emissions were captured at the engine exit plane using three particle (N₂-diluted) and three gas (undiluted) probes mounted within a water-cooled probe rake. The probe rake was placed near the center and approximately 33 cm from the engine exhaust plane to capture representative samples and avoid diluting with surrounding air. The rake was mounted on a 15-cm-diam, 1.23-m-long stainless steel post supported on a stand restrained with the engine test bed. The particle and gas probes had nominal port diameters of 1.6 and 1.5 mm, respectively. The probes types were alternated within the rake and separated by 3.18 cm center to center (Fig. 1). The exhaust gas temperature was monitored using a thermocouple installed in a blank probe, and the exhaust pressure was measured using an open probe connected to a pressure gauge in the TERTEL. The aerosol sample was diluted with nitrogen (at room temperature) at the probe tip to minimize condensation of water and organic species and to minimize particle loss to the tubing walls. Although the dilution ratios were set using high-precision Brooks Instrument 5850i (0–10 slpm) flow controllers, the dilution ratios used for particle number (PN) and mass correction were determined by the ratio of the carbon dioxide (CO₂) concentration of the diluted and undiluted streams. The average of CO₂ measurements from two separate probes, typically within $\pm 10\%$ (95% confidence), was used for the calculations. Dilution ratios were between 8 and 50:1, with higher dilutions required at higher engine power. Emission samples were transported from the probe rake to a heated valve box using 6.35-mm-o.d., 4.6-mm-i.d. heated lines (150°C). Samples from each probe could be sent to the desired instrument by means of fast-response ball valves within the box (also maintained at 150°C). Since the required sample dilution varied based on the analytical instrument, two six-way valves with three dilution schemes (diluted for PN and TEOM, undiluted for the smoke sampler) were used to provide the required dilution to the appropriate probe. Undiluted and diluted particle samples were kept at 150 and 75°C, respectively, from the valve box to the instruments to help maintain sample integrity. The total length of the heated sample lines from the probe stand to the instruments was approximately 23 m. The emissions samples were drawn into the instruments via vacuum pumps. A simplified flow diagram of the sampling system is shown in Fig. 2.

Jet Fuel Characteristics

JP-8 is Jet A-1 commercial aviation fuel with a military additive package that includes a fuel system icing inhibitor (FSII) at ~1000–1500 ppm, corrosion inhibitor/lubricity enhancer at

[†]Data available online at <http://www.tsi.com> [retrieved 11 April 2008].

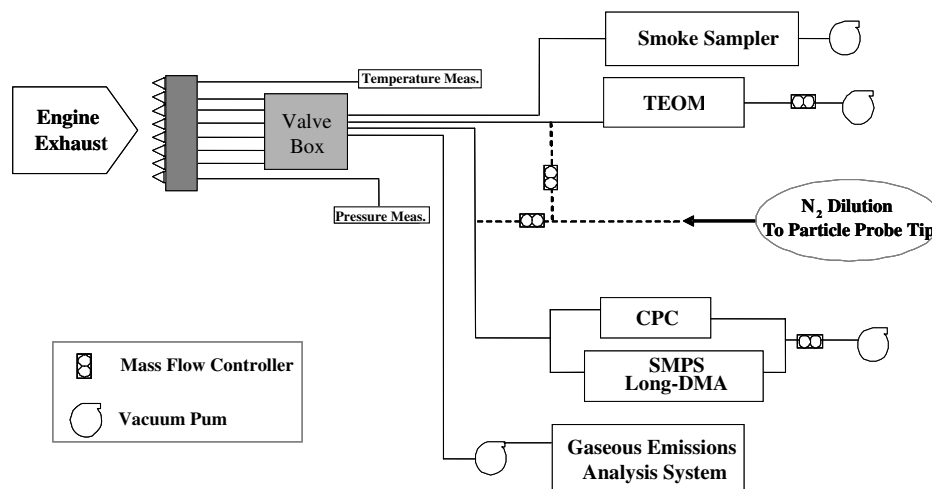


Fig. 2 Simplified emissions sampling system.

~20 ppm, and a static dissipater additive at ~5 ppm. JP-8 contains hundreds of different types of hydrocarbons. In a typical JP-8 fuel, branched (iso) and normal (*n*) paraffins account for approximately 60% of the total hydrocarbons. The *n* paraffins typically range from *n*-octane (*n*-C₈) to *n*-hexadecane (*n*-C₁₆), with maximum concentrations from *n*-decane (*n*-C₁₀) to *n*-dodecane (*n*-C₁₂). JP-8 also contains approximately 20% mono-, di-, and tricycloparaffins. Aromatics are the other significant fraction (~15–20%) of JP-8 fuel. The alternative fuel used in this study was produced by Syntroleum Corporation from natural gas via the FT process. Extensive details on this fuel have been previously provided [6,7,10]. The fuel is comprised solely of iso (82%) and normal (18%) paraffins with a distillation (i.e., molecular weight) range consistent with that typically observed for an aviation fuel. The isoparaffins in this fuel are mainly monomethyl-substituted species. The chemical composition of fuels was determined using a variety of chromatographic techniques, including GC/MS and high-performance liquid chromatography. ASTM International specification conformance tests [11–22] were conducted to verify fuel compliance with all JP-8 specifications and to determine the concentration of known PM precursor species, such as aromatics and sulfur. Table 1 shows the specification limits of several JP-8 properties and the properties of the JP-8 and FT fuel used in this effort. This FT fuel conforms to the recently released specifications for SPK, which can be blended up to 50 vol % with JP-8 and was recently certified on B-52 platforms [23].

Table 1 ASTM specification test results for JP-8 and FT fuels used during tests

ASTM test	Standard	JP-8	FT fuel
Aromatics, vol % (D1319 [11])	Max 25.0	19.2	0
Total sulfur, wt % (D4294 [12])	Max 0.30	0.140	0
Initial boiling point, °C (D86 [13])	Report	173	150
10% Recovered, °C (D86 [13])	Max 205	189	173
20% recovered, °C (D86 [13])	Report	192	181
50% recovered, °C (D86 [13])	Report	207	208
90% recovered, °C (D86 [13])	Report	234	245
Final boiling point, °C (D86 [13])	Max 300	248	258
Distillation-residue, vol % (D86 [13])	Max 1.5	1.3	1.5
Loss, %vol (D86 [13])	Max 1.5	1.5	0.5
Freeze point, °C (D5972 [14])	Max -47	-51	-49
Existent gum, mg/100ml (D381 [15])	Max 7.0	1.1	0.6
Viscosity at -20°C, cSt (D445 [16])	Max 8.0	5.0	4.9
FSII (DiEGME), vol % (D5006 [17])	0.10–0.15	0.12	0.05
Smoke point, mm (D1322 [18])	Min 19.0	25	35
Flash point, °C (D93 [19])	Min 38	62	63
Specific gravity at 15.5°C (D4052 [20])	0.775–0.840	0.806	0.756
Heat of combustion, Btu/lb (D3338 [21])	Min 18,400	18,500	18,980
Hydrogen content, % mass (D3343 [22])	Min 13.4	13.7	15.3

Test Conditions

The test plan for this campaign is shown in Table 2. A total of 30 test runs were conducted. All three engines (one T700 and two T701C) were operated on JP-8 at three power settings: ground idle (or idle), 75%-maximum power, and maximum power. One cycle consisted of consecutive tests at the three conditions. Four cycles were run for the T700 and two for each T701C. For the second T701C, two cycles were also performed with the FT fuel. The engine was operated at each power setting for approximately 30 min to acquire multiple measurements from two probe locations. The tests were conducted in the test sequence shown, i.e., from low to high power. The engine conditions were set by controlling the turbine rotational speed. For tests with the neat FT fuel, the fuel was stored in an external tank and supplied to the engine fuel pump via an air-driven diaphragm pump.

Test Results and Discussion

Engine Operation

The engines were observed to operate normally during the tests. As anticipated, no discernible difference in engine operation (performance parameters were within measurement variability) was observed between JP-8 and neat FT fuel. After test completion with the FT fuel, the engine was thoroughly inspected and no anomalies were found. The total engine run time with the neat FT fuel was approximately 2.5 h.

Table 2 Test plan for emissions tests on T700 and T701C engines

Test run	Power setting
T700 with JP-8	
1,4,7,10	Ground idle
2,5,8,11	75%
3,6,9,12	Max
T701C-1 with JP-8	
13,16	Ground idle
14,17	75%
15,18	Max
T701C-2 with JP-8	
19,22	Ground idle
20,23	75%
21,24	Max
T701C-2 with FT	
25,28	Ground idle
26,29	75%
27,30	Max

Particulate-Matter Emissions

Particle Number

PN emissions were quantified with a CPC and corrected for dilution based on the CO_2 measurement of the diluted and raw samples. Dilution ratios ranged from an average of 8:1 at idle to 50:1 at maximum power. Higher dilution was required to maintain the particle counts within the CPC measurement range. Particle-number emission indices (PN-EIs), the number of particles produced per unit mass of fuel consumed, were calculated using the following relationship derived from fluid flow fundamentals:

$$\text{PN-EI} = 2.833 \times 10^3 \times \text{PN}_{\text{corrected}} \times (1 + F/A)/(F/A) \times T/P \quad (1)$$

where PN-EI is the number of particles per kilogram of fuel, $\text{PN}_{\text{corrected}}$ is the dilution-corrected PN in number of particles per cubic centimeters, T is the sample temperature at the instrument in Kelvin (~ 293 K), P is the sample pressure at the instrument in atmospheres, F/A is the engine fuel-to-air ratio, and 2.833×10^3 is a unit conversion factor.

The engine F/A ratios were determined based on the CO and CO_2 emissions following the SAE ARP 1533A guidelines [24]. The average PN-EI (not corrected for sample line losses) varied from 1.25×10^{15} at idle to 4.12×10^{15} #/kg fuel at maximum continuous power for the T700 and 4.56×10^{14} to 2.11×10^{15} #/kg fuel for the T701C. The PN uncertainty for each individual test run was excellent at less than $\pm 8\%$ (95% confidence), reflecting the steadiness of the engine operation. The average PN-EI corrected for estimated line losses are shown in Fig. 3. The losses are based on an unreported in-house study designed to quantify particle line losses through the 23 m heated line and valving system used in this campaign. The in-house study (conducted using particulate exhaust from a T63 helicopter engine) showed average losses between ~ 40 – 60% in PN (depending on engine condition) for particulate emissions, with a similar size-distribution range as for the T700 engines. The reported values in Fig. 3 represent averages of multiple runs from two probes. The uncertainty for each average value varied depending on engine condition. At idle, the average uncertainty was higher ($\pm 25\%$) than at both the 75%-maximum ($\pm 12\%$) and maximum power ($\pm 10\%$) conditions. Higher uncertainties at the idle condition are likely due to the higher concentrations of unstable volatile and semivolatile species at the lower power setting. The physical properties of these species are believed to be extremely sensitive to temperature and pressure, and therefore any small change in these may affect gas-to-particle conversion processes in the sampling system, which subsequently influence the number of particles measured. For the higher power settings, the concentration of semivolatile species (i.e., organic carbon) is significantly reduced and particles are more stable, which reduces the data variation. It was observed that the difference between the PN measurements from the two individual probes

(separated by 6.4 cm) was also highly dependent on engine condition. This difference was larger at idle ($\sim 40\%$) than at both the 75%-maximum ($\sim 20\%$) and maximum power ($\sim 13\%$) conditions. However, the trends observed for samples from both probes were consistent for all power settings and engines. The relatively small difference in PN at higher power demonstrates the fairly uniform PM profile in the exhaust. As shown in Fig. 3, the PN-EI varied directly with engine power at an average of 3.0 – 6.9×10^{15} #/kg fuel for the T700 and significantly lower 1.1 – 3.5×10^{15} #/kg fuel for the T701C operating on conventional JP-8 fuel. For the T701C engine operating with FT fuel, lower particle emissions for all conditions were evident. Reductions of 40–97% in PN-EI were observed with the FT fuel, with the highest reductions occurring at engine idle. The higher impact at idle is likely due to the smaller particles produced at this condition and the production of even smaller and more easily oxidized particles with the FT fuel. The lower PM emissions with the FT fuel are primarily due to its aromatic-free nature. Aromatics are known soot precursors that act as seeds for the growth of PAHs, which subsequently nucleate into soot particles. The propensity of aromatics to produce soot has been demonstrated in large-scale combustors and laboratory flames. A summary of several efforts and the role of aromatics in soot formation have been presented by Richter and Howard [25]. Reduction in the fuel aromatic content decreases precursors that contribute to the formation of soot nuclei. The FT fuel is comprised solely of normal and branched paraffinic compounds, which are believed to produce soot primarily via fragmentation and polymerization reactions, which are much slower (i.e., less efficient) than condensation reactions with aromatics [26]. Reductions in PM emissions with FT fuels have been observed previously in a T700 engine and other test platforms [6–8]. Because of the sampling methodology employed, most of the PM measured are nonvolatile (mostly soot) particles; therefore, the lack of sulfur in the FT fuel did not have a significant impact on the measured particle reductions observed here. However, significant reductions in volatile particles (which nucleate as the exhaust is cooled and mixed in the atmosphere) are anticipated, as most of these are sulfur-based.

Particle Size Distributions

Particle size distributions of the PM emissions were measured over a range of 7–300 nm in aerodynamic mobility diameter. The average particle size distributions for operation of both engines with JP-8 for the power settings evaluated are shown in Fig. 4. The y axis is represented by $dN/d\log D_p$ (a size-bin normalized particle number), which is a common practice in aerosol measurements to remove artificial counts due to the raw nonuniform voltage settings used in the DMA. Each curve represents the average of a minimum of eight size-distribution scans (four per probe). Data reproducibility for each power setting was excellent at maximum and 75%-maximum settings, with averages of ± 7 and 15% (1σ), respectively, but relatively poor at idle power ($\pm 40\%$). As discussed in the

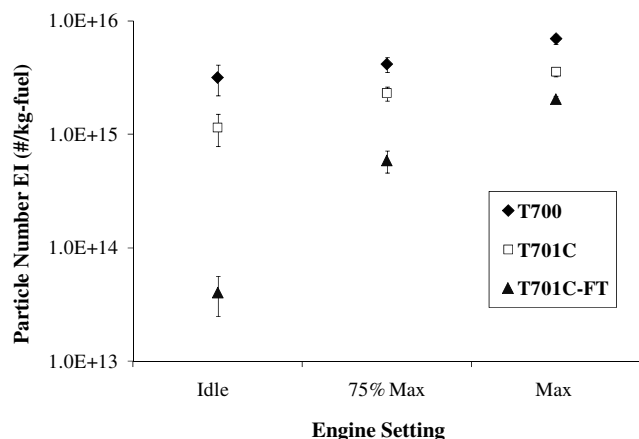


Fig. 3 Particle-number emission indices at three power settings for T700 and T701C engines operating with JP-8 and the T701C operating with FT fuel.

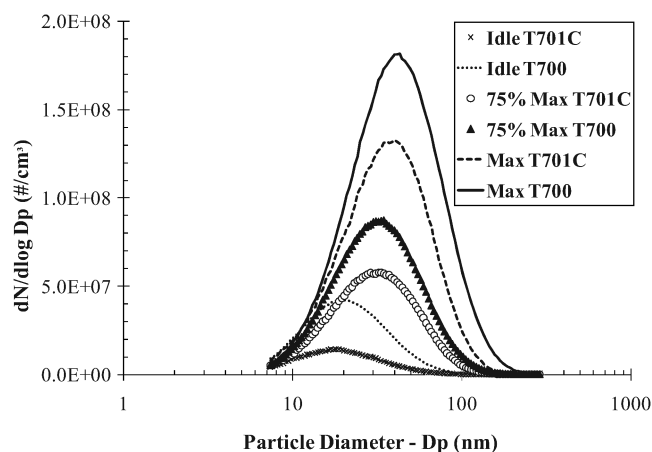


Fig. 4 Particle size distributions of PM emissions from T700 and T701C engines operated with JP-8 at three power settings.

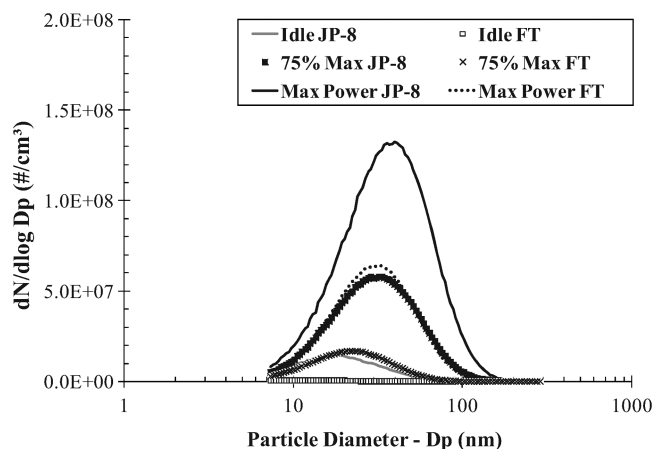


Fig. 5 Particle size distributions of PM emissions from T701C engine operated with JP-8 and FT fuel at three power settings.

previous section, the poorer PN repeatability at low power is likely due to the higher concentration of semivolatile (organic) particles in the exhaust. Size-distribution curves for both engines and for all three conditions are observed to follow a single-mode lognormal distribution with average geometric mean diameters of approximately 21 nm for idle, 30 nm for 75%-maximum power, and 37 nm for maximum power. Although the particle concentrations were significantly lower for the T701C compared with the T700, the average particle diameters for both engines were very similar. The particle mean diameters for both engines were approximately 24, 35, and 42 nm from low to high power.

Comparison of the particle size distributions of the T701C with the JP-8 (solid symbols) and FT (open symbols) fuels is shown in Fig. 5. Consistent with the particle-number data, dramatic reductions in particle concentrations (magnitude of size-distribution peak) are observed with the FT fuel. Additionally, average reductions of 25% in the mean particle diameter were observed with the FT fuel at all conditions. The reduced particle mean diameter is the result of fewer soot nuclei available for surface growth (by agglomeration and aggregation) as a consequence of the lower concentration of soot precursors in the fuel (aromatics). These trends are consistent with previous FT emissions tests in engines and combustors [6,7].

PM Mass Emissions

Engine PM mass emissions were measured online using a TEOM and offline via temperature programmed oxidation (carbon burn-off) of soot samples collected on quartz filters. Mass measurements with the TEOM varied significantly at idle, in which uncertainties up to $\pm 75\%$ (95% confidence) were observed. The high error at low engine power is primarily due to the relatively low particulate load and insufficient sensitivity of the TEOM. For the 75%-maximum and maximum power settings, the uncertainty was significantly reduced to an average of $\pm 15\%$ (95% confidence). The TEOM PM mass-EI was calculated in a manner similar to that used for the PN-EI:

$$\text{PM mass-EI} = 2.83 \times 10^{-6} \times \text{PM mass}_{\text{conc}} \times \frac{1 + F/A}{F/A} \times \frac{T}{P} \quad (2)$$

where PM mass-EI is the grams of PM per kilogram of fuel, PM mass_{conc} is dilution-corrected PM mass concentration in mg/m^3 , T is the standard temperature (293 K), P is the sample pressure at the instrument in atmospheres (1 atm), F/A is the engine fuel-to-air ratio, and 2.83×10^{-6} is a unit conversion factor.

The PM mass-EI varied directly with power setting and ranged (uncorrected for losses) from 0.053 to 1.04 g/kg fuel for the T700 and from 0.049 to 0.49 g/kg fuel for the T701C with JP-8. The PM-EIs corrected for estimated line losses (25% at high power and 60% at idle, determined from in-house experiments) ranged from 0.2–1.4 g/kg fuel for the T700 and from 0.2–0.6 g/kg fuel for the T701C. The PM mass-EIs as a function of engine power setting are

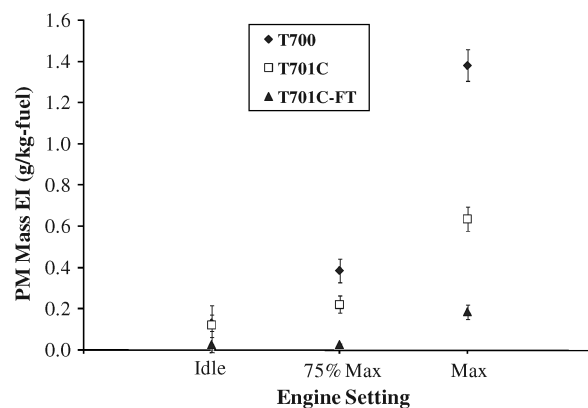


Fig. 6 Measured particulate-matter mass emission indices for T700 and T701C engines using a TEOM.

shown in Fig. 6. As shown, the trends of PM mass-EIs as a function of power are similar to those of the PN-EI. It is noted that the PM mass-EIs for the T700 engine are significantly lower than those reported by Wade [27] for a T700 engine, which ranged between 1.5–2.6 g/kg fuel for the same range of engine conditions. Differences in the measurement techniques may explain the disagreement between the PM mass measurements. Compared with PM mass emissions of military engines tested recently (T56 and TF33) under this SERDP project, both the T700 and T701C engines produced significantly lower PM emissions [7,28].

Carbon mass measurements via the carbon burnoff method (LECO) showed significantly higher fractions of OC at engine idle, compared with the higher power settings. Average ratios of organic carbon to total carbon (OC/TC) of 0.41, 0.28, and 0.16 were observed for idle, 75%-maximum, and maximum power, respectively, for the engines operating with JP-8. For the T701C with FT fuel, the OC/TC ratios averaged 0.40, 0.37, and 0.27, which were moderately higher than those observed with JP-8 for the two high-power cases. However, it should be noted that although the OC/TC ratios were higher for the FT fuel, the absolute OCs were lower for the FT; thus, the lower OC/TC for the FT were due to the significant decrease in soot formation. As with the TEOM, the mass measurements with the LECO were highly variable at low engine power.

Comparison of the mass concentration measurements determined using the TEOM and LECO is shown in Fig. 7. The error bars represent one standard deviation based on a minimum of three measurements. The LECO measured mass was observed to be significantly higher (up to 7.2 times) than for the TEOM for engine idle (PM mass < ~ 2.0). The high concentrations of OC at low power combined with the ineffectiveness of the TEOM to quantify the OC mass and lack of instrument sensitivity for these low-mass loadings

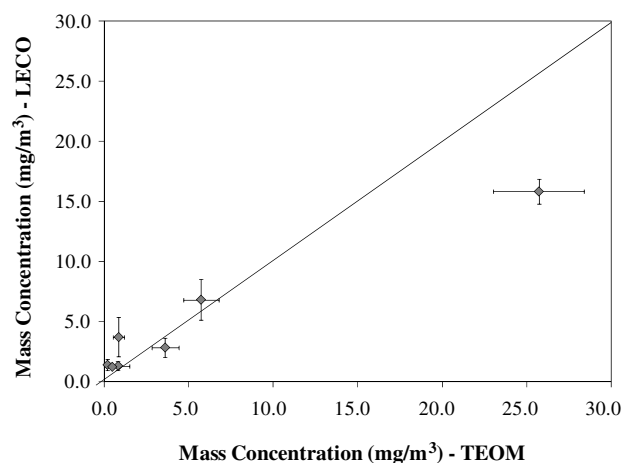


Fig. 7 Comparison of particulate-matter mass concentration measured online with a TEOM and offline via carbon oxidation using a LECO RC-412 multiphase carbon analyzer.

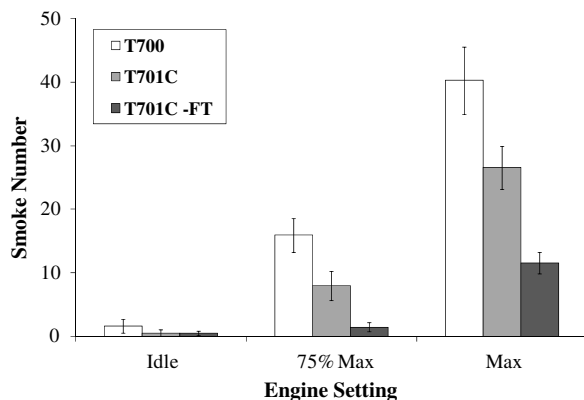


Fig. 8 Smoke numbers for T700 and T701C engines operated with JP-8 at three power settings and data for the T701C operating on the FT fuel.

are believed to be the cause for the large discrepancies. These results suggest that at low engine power, where there is a higher fraction of unburned hydrocarbons (i.e., OCs), the TEOM may underestimate the total particle mass. For the two high-power cases, the agreement between the two techniques is significantly better because of the higher total mass and increased elemental carbon; however, significant discrepancies are still observed. For the higher-mass concentrations (maximum power), the TEOM measurement is 1.6 to 2.1 times higher than the LECO. Differences in filter efficiency between the two instruments may explain the discrepancy between the two techniques. In addition, the TEOM sample was diluted, whereas the LECO sample was undiluted; error due to sample dilution correction can also affect the measured value. Overall, further research is warranted to understand the discrepancies between these techniques in order to develop a reliable methodology for PM mass measurement.

Smoke Number

Engine smoke numbers (SNs) were measured following SAE ARP 1179 [9]. The SN measures the relative difference in filter reflectance between a clean (unused) and stained (test) filter. Average SNs (minimum of eight samples per engine condition) for all test conditions are shown in Fig. 8. As anticipated, the SN varied directly with engine power. At idle, the SNs were essentially zero for both engines and fuels. At maximum power, average SNs of 40 were observed for the T700, whereas significantly lower SNs were observed for the T701C operating on both JP-8 and FT fuel. The average SNs for the T701C were approximately 40% lower than those for the T700, and average reductions of 65% were observed for the T701C when operated with the FT fuel. The SN trends as a function of engine, fuel, and power setting agree qualitatively with the PN-EI trends.

Analysis of PAHs from Soot Samples

Soot samples collected on quartz filters were analyzed to preliminarily investigate potential differences in the quantity and type of PAH compounds absorbed onto the particulate samples. Samples were prepared for analysis using ultrasonic extraction with methylene chloride and were analyzed via GC/MS to quantify PAH compounds and evaluate the impact of engine type, power setting, and fuel on the relative and absolute formation [7]. Using this

technique with the limited available sample quantities, only fluoranthene and pyrene were above the quantifiable detection limit. Results in nanograms (ng) of PAH per m³ of exhaust gas volume are shown in Table 3. Larger and smaller PAHs are likely present in the samples but could not be detected with the sampling and analytical techniques employed here. As shown in Table 3, the total PAH concentration increased with increasing power setting, whereas the more efficient T701C engine and FT fuel both produced lower PAH emissions. These results were expected, as PAHs are believed to be intermediates in the soot-formation pathway, and the trends follow those observed for the overall soot mass and PM emissions. An attempt was made to normalize the PAH quantity to the mass of soot collected to provide insight into the relative selectivity of PAH formation in the soot-formation process (e.g., a lower ratio for FT fuel would imply an alternate pathway for soot formation rather than being solely due to reduced overall formation rate.) However, this analysis was inconclusive due to the limited available samples for analysis. Future efforts will be made to improve the sensitivity of the PAH detection and to provide additional samples for better statistical analysis.

Gaseous Emissions

Carbon Monoxide and Nitrogen Oxides

Gaseous emissions were quantified with an FTIR-based gas analyzer. As criteria pollutants, only CO and NO_x emissions are discussed in detail. Average CO and NO_x EIs for the T700 and T701C engines as a function of power setting are shown in Figs. 9 and 10. The CO-EIs ranged from 2.3–53.7 g/kg fuel for the T700 and from 2.8–31.0 g/kg fuel for the T701C. These CO-EIs are in excellent agreement with previous T700 engine emissions tests by Jones et al. [8] and Wade [27]. The NO_x-EIs ranged from 2.0–9.9 g/kg fuel for the T700 and from 2.8–15.0 g/kg fuel for the T701C. As anticipated, the engines produced higher CO and lower NO_x emissions at the lower power conditions as a result of the lower engine efficiency and exhaust temperatures, respectively. The T700 generated nearly twice the CO emissions as the T701C, which reflects a higher combustion efficiency for the latter. The approximately 40% higher NO_x emissions of the T701C over the T700 is the result of the higher-performance and higher-operating-temperature capabilities of the T701C. As anticipated, operation with the FT fuel rendered negligible differences in NO_x, since the production of these are temperature-driven and not significantly influenced by fuel type. The CO emissions for the T701C were only slightly reduced (~5–10%) with the FT fuel.

Analysis of Aldehydes

Aldehydes are produced during the combustion of hydrocarbons, and several have been identified as toxic compounds. Analysis of aldehydes was performed to determine the EIs and to assess any differences in their formation between the FT and JP-8 fuels. The analysis of aldehydes was performed using the MKS FTIR-based analyzer and a modified EPA Compendium Method TO-11A [29]. For the latter, silica-gel cartridges (Supelco, part number H30, 1 g bed weight) treated with 2,4-dinitrophenylhydrazine (DNPH) were used to capture and derivatize aldehydes from the engine exhaust and ambient air. In this analysis, 1 slpm of engine exhaust was sampled through the ambient-temperature silica-gel cartridge. Aldehydes in the gas sample reacted with the derivatizing agent to form aldehyde-diphenylhydrazone. The cartridges were capped and placed into

Table 3 Concentrations of measurable PAHs for operation of the T700 and T701C engines as a function of power setting and fuel type

Engine/fuel	Fluoranthene, ng/m ³			Pyrene, ng/m ³		
	Idle	75%	Max	Idle	75%	Max
T700-JP-8	— ^a	9.6E + 03	2.3E + 04	4.2E + 02	2.0E + 04	5.0E + 04
T701C-JP-8	— ^a	3.6E + 03	2.1E + 04	— ^a	9.4E + 03	4.1E + 04
T701C-FT	— ^a	— ^a	3.5E + 03	— ^a	3.5E + 02	9.0E + 03

^aDenotes below the detection limit.

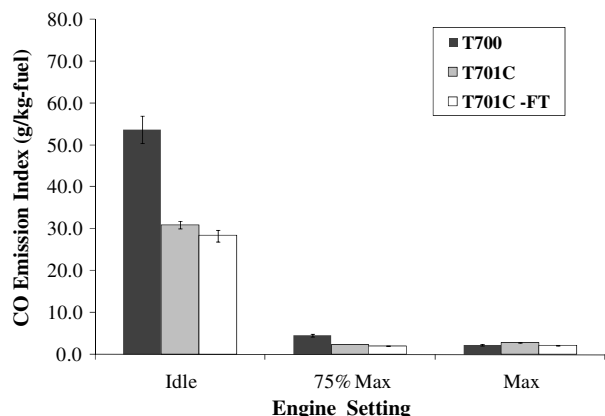


Fig. 9 CO Emission Indices at three power settings for T700 and T701C engines operating with JP-8 and the T701C operating with FT fuel.

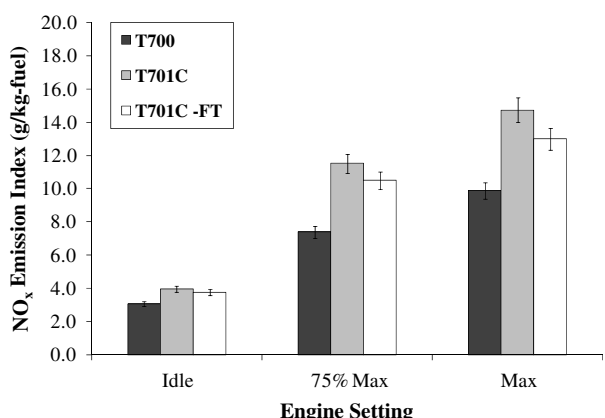


Fig. 10 NO_x emission indices at three power settings for T700 and T701C engines operating with JP-8 and the T701C operating with FT fuel.

foil-lined bags in coolers for transport from the field. The cartridges were subsequently treated with 10 ml of acetonitrile to extract the derivatized aldehydes; the extracts were analyzed by GC/MS using a DB5-MS column, operating in the selected ion-monitoring mode. Quantification ions were selected based on the most abundant and unique ions for each of the components. Standard solutions of all aldehydes were prepared and analyzed to develop a calibration range between 0 and 15 mg/liter of each derivatized aldehyde. Comparison to the calibration standards was performed to quantify the mass of each aldehyde per volume of gas.

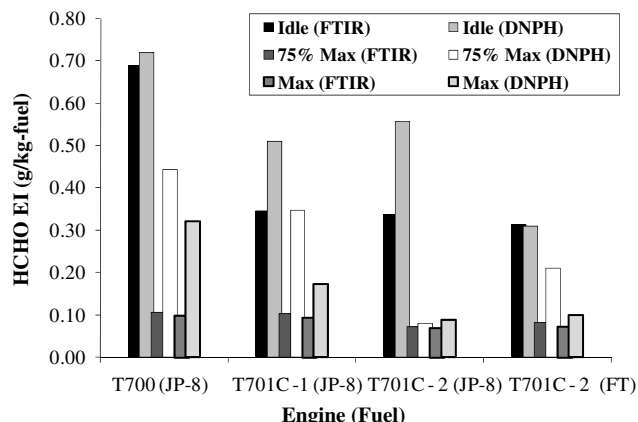


Fig. 11 Formaldehyde emission indices for T700 and T701C engines using a modified EPA Compendium Method TO-11A (DNPH) [29] and an FTIR-based analyzer.

Tests results show that formaldehyde (HCHO) was the only aldehyde produced at quantities above the sensitivity of this technique (~ 0.1 ppm). Figure 11 displays the HCHO emission indices using both analytical methods for the three engines with JP-8 and the T701C with FT fuel. The average errors were $\pm 25\%$ (1σ) and $\pm 10\%$ (1σ) for the DNPH and FTIR measurements, respectively. The average HCHO-EIs ranged from 0.50 g/kg fuel at idle to 0.13 g/kg fuel at maximum engine power. Relatively good agreement (within uncertainty) is observed between the measurement techniques at the idle condition, in which the concentrations were largest. At the 75%-maximum and maximum power conditions, large discrepancies between the methods are likely the result of their reduced concentration and lack of measurement sensitivity. The T700 produced significantly higher concentrations of HCHO at the idle condition, compared with the T701C. All HCHO measurements with the FTIR and DNPH methods (except the 75%-maximum DNPH) show that operation of the T701C with the FT fuel had minimal impact on the production of HCHO.

Conclusions

Aircraft have been identified as significant sources of local pollution at airports and military bases. Accurate determination of emission indices from aircraft is necessary to assess their environmental impact in order to take appropriate action. In this effort, conventional aerosol instruments and an FTIR-based gas analyzer were used to measure the particulate matter (PM) and gaseous emissions of three T700 series engines (one T700 and two T701C), to determine emission indices and to assess the validity and performance of the instrumentation and measurement techniques. In general, the aerosol instrumentation and sampling methodology employed provided consistent and reliable measurements throughout the test campaign. Test results show that the T701C engine emitted significantly lower soot emissions than the T700 for all conditions tested. Corrected PM mass emission indices ranged from 0.2–1.4 g/kg fuel for the T700 and from 0.2–0.6 g/kg fuel for the T701C. Particle number and smoke numbers trends are consistent with those of the PM mass-EI. Excellent agreement in PM emissions measurements were observed between the two T701C engines. Slightly higher NO_x and lower CO emissions were observed for the T701C compared with the T700, which demonstrates higher operation temperatures and combustion efficiency for the T701C. Consistent with previous studies on TF33 and T63 engines, the FT fuel significantly reduced soot emissions (~ 40 – 97% in particle number), with smaller mean particle sizes and minimum impact on gaseous emissions, compared with operation on JP-8. The reduction in PM emissions is largely attributed to the lack of aromatic compounds in the FT fuel.

Acknowledgments

This work was funded by the Department of Defense Strategic Environmental Research and Development Program (SERDP) office within the Weapon Systems and Platforms focus area under the Project WP-1401 led by Oak Ridge National Laboratory (ORNL). ORNL is managed by UT-Battelle, LLC, for the U.S. Department of Energy under contract DE-AC05-00OR22725. The work of the University of Dayton Research Institute (UDRI) was supported by the U.S. Air Force Research Laboratory (AFRL) under the cooperative research agreement F33615-03-2-2347. Special thanks to Joe Lukas from the Aviation Branch Maintenance Division at Fort Stewart for his support and coordination of these tests and to Daniel Houck, Robert Henson, Jason Mikelonis, and Robert Shell for operating the test facility. The authors are also very grateful to Joe Mantz from UDRI and Tom Greene from Taitech, Inc., for their technical support during the tests and to Linda Shafer and Rhonda Cook of UDRI for the polycyclic aromatic hydrocarbon analysis.

References

- [1] "For Greener Skies-Reducing Environmental Impacts of Aviation," Committee on Aeronautics Research and Technology for Environmental Compatibility, National Research Council, 2002.

- [2] Anderson, B. E., Branham, H.-S., Hudgins, C. H., Plant, J. V., Ballenthin, J. O., Miller, T. M., et al., "Experiment to Characterize Aircraft Volatile Aerosol and Trace-Species Emissions (EXCAVATE)," NASA TM-2005-213783, 2005.
- [3] Wey, C. C., Anderson, B.E., Hudgins, C., Wey, C., Li-Jones, X., Winstead, E., et al., "Aircraft Particle Emissions eXperiment (APEX)," NASA TM 2006-214382, 2006.
- [4] "Non-Volatile Particle Exhaust Measurement Techniques," SAE International, Aerospace Information Report, SAE AIR 5892, Warrendale, PA, 2004.
- [5] Kelly, K. E., Sarofim, A. F., Lighty, J. S., Wagner, D. A., Arnott, W. P., Rogers, C. F., Zielinska, B., and Prather, K. A., "User Guide for Characterizing Particulate Matter. Evaluation of Several Real-Time Methods," College of Engineering, Univ. of Utah, Salt Lake City, UT, 1 Oct. 2003.
- [6] Corporan, E., DeWitt, M. J., Belovich, V., Pawlik, R., Lynch, A. C., Gord, J. R., and Meyer, T. R., "Emissions Characteristics of a Turbine Engine and Research Combustor Burning a Fischer-Tropsch Jet Fuel," *Energy and Fuels*, Vol. 21, No. 5, 2007, pp. 2615–2626. doi:10.1021/ef070015j
- [7] Corporan, E., DeWitt, M. J., Klingshirn, C. D., and Striebich, R. C., "DoD Assured Fuels Initiative: B-52 Aircraft Emissions Burning a Fischer-Tropsch/JP-8 Fuel Blend," *Proceedings of the 10th International Conference on Stability and Handling of Liquid Fuels* [CD-ROM], International Association for Stability, Handling and Use of Liquid Fuels, Atlanta, 2007.
- [8] Jones, X. L., Penko, P.F., Williams, S., Moses, C., "Gaseous and Particle Emissions in the Exhaust from a T700 Helicopter Engine," ASME International Turbo Expo Conference, ASME International, Paper GT2007-27522, 2007.
- [9] "Aircraft Gas Turbine Exhaust Smoke Measurement," SAE Aerospace Recommended Practice, Rept. SAE ARP 1179. Society of Automotive Engineers, Warrendale, PA, 1970.
- [10] DeWitt, M. J., Striebich, R., Shafer, L., Zabarnick, S., Harrison, W. E., III, Minus, D. E., and Edwards, T., "Evaluation of Fuel Produced via the Fischer-Tropsch Process for Use in Aviation Applications," American Institute of Chemical Engineers, Spring National Meeting, Paper 58b, 2007.
- [11] "Standard Test Method for Hydrocarbon Types in Liquid Petroleum Products by Fluorescent Indicator Adsorption," ASTM International, Std. ASTM D1319, Alexandria, VA, Oct. 2008.
- [12] "Standard Test Method for Sulfur in Petroleum and Petroleum Products by Energy Dispersive X-Ray Fluorescence Spectrometry," ASTM International, Std. ASTM D4294, Alexandria, VA, Oct. 2008.
- [13] "Standard Test Method for Distillation of Petroleum Products at Atmospheric Pressure," ASTM International, Std. ASTM D86, Alexandria, VA, April 2007.
- [14] "Standard Test Method for Freezing Point of Aviation Fuels (Automatic Phase Transition Method)," ASTM International, Std. ASTM D5972, Alexandria, VA, Nov. 2005.
- [15] "Standard Test Method for Gum Content in Fuels by Jet Evaporation," ASTM International, Std. ASTM D381, Alexandria, VA, Nov. 2004.
- [16] "Standard Test Method for Kinematic Viscosity of Transparent and Opaque Liquids (and Calculation of Dynamic Viscosity)," ASTM International, Std. ASTM D445, Alexandria, VA, May 2006.
- [17] "Standard Test Method for Measurement of Fuel System Icing Inhibitors (Ether Type) in Aviation Fuels," ASTM International, Std. ASTM D5006, Alexandria, VA, Dec. 2003.
- [18] "Standard Test Method for Smoke Point of Kerosene and Aviation Turbine Fuel," ASTM International, Std. ASTM D1322, Alexandria, VA, June 1997.
- [19] "Standard Test Methods for Flash Point by Pensky-Martens Closed Cup Tester," ASTM International, Std. ASTM D93, Alexandria, VA, May 2007.
- [20] "Test Method for Density, Relative Density, and API Gravity of Liquids by Digital Density Meter," ASTM International, Std. ASTM D4052, Alexandria, VA, April 1996.
- [21] "Standard Test Method for Estimation of Net Heat of Combustion of Aviation Fuels," ASTM International, Std. ASTM D3338, Alexandria, VA, May 2008.
- [22] "Standard Test Method for Estimation of Net Heat of Combustion of Aviation Fuels," ASTM International, Std. ASTM D3343, Alexandria, VA, Nov. 2005.
- [23] "Turbine Fuel, Aviation, Kerosene Type, JP-8 (NATO F-34), NATO F-35, and JP-8+100 (NATO F-37)," U.S. Dept. of Defense, MIL-DTL-83133F, 11 April 2008.
- [24] "Procedure for the Analysis and Evaluation of Gaseous Emissions from Aircraft Engines," Aerospace Recommended Practice SAE ARP 1533A, SAE International, Warrendale, PA, 2004.
- [25] Richter, H., and Howard, J. B., *Progress in Energy and Combustion Science*, Vol. 26, Nos. 4–6, 2000, pp. 565–608. doi:10.1016/S0360-1285(00)00009-5
- [26] Lefebvre, A. H., *Gas Turbine Combustion*, 1st ed., McGraw-Hill, New York, 1983, Chap. 11.
- [27] Wade, M. D., "Aircraft/Auxiliary Power Units/Aerospace Ground Support Equipment Emission Factors," U.S. Air Force Rept. IERA-RS-BR-SR-2003-0002, 2004.
- [28] Corporan, E., Quick, A., and DeWitt, M. J., "Characterization of Particulate Matter and Gaseous Emissions of a C-130H Aircraft," *Journal of the Air & Waste Management Association*, Vol. 58, No. 4, April 2008, pp. 474–483. doi:10.3155-1047-3289.58.4.474
- [29] "Compendium Method TO-11A: Determination of Formaldehyde in Ambient Air Using Adsorbent Cartridge Followed by High Performance Liquid Chromatography (HPLC) [Active Sampling Methodology]," Compendium of Methods for the Determination of Toxic Organic Compounds in Ambient Air, 2nd ed., Center for Environmental Research Information, U.S. Environmental Protection Agency, Rept. EPA/625/R-96/010b, Cincinnati, OH, www.epa.gov/ttn/amtic/files/ambient/airtox/to-11a.pdf [retrieved 21 March 2008].

A. Gupta
Associate Editor